

Conformational Dynamics of 8-Oxoguanine Mispairing Reveal a Mechanism of Polymerase λ Misincorporation

G. Ferguson¹, L. Slocombe², M. Winokan³, B. Howlin¹, and M. Sacchi¹

¹*Department of Chemistry and Chemical Engineering, University of Surrey, Guildford, GU2 7XH, UK.*

²*Beyond Center for Fundamental Concepts in Science, Arizona State University, Tempe, Arizona 85287-0506, United States.*

³*Diamond House, Harwell Science and Innovation Campus, Fermi Ave, Didcot OX11 0DE*

September 22, 2025

1 Abstract

Experimental evidence has shown the stability of oxygen-stress-damaged guanine, known as 8-oxoguanine. This common oxygen-damaged nucleobase is often found in the presence of reactive oxygen species and can result in the mispairing between adenine and 8-oxoguanine in a Hoogsteen pair. We have computationally investigated the role of 8-oxoguanine to support experimental results and focus the investigation towards the polymerase structure, identifying how 8-oxoguanine interacts in the polymerase environment. Quantum mechanical investigations show the Hoogsteen pairing of adenine and 8-oxoguanine is the most energetically favourable state compared to a Watson-Crick state, supporting experimental evidence. Molecular Dynamical calculation of 8-oxoguanine located in B-DNA provide an average C1' backbone spacing of 1.1 nm compared to adenine - thymine spacing of 1.05 nm but remains within the error margin, however when in the polymerase environment, 8-oxoguanine and the canonical adenine - thymine spacing match at 1.11-1.12nm spacing while 8-oxoguanine is located on the template strand, but is disrupted by tyrosine 251 while situated on the triphosphate strand. We observe that 8-oxoguanine, when paired with adenine in polymerase λ , can mimic the adenine-thymine structure, as predicted in experimental results, and thus would be misincorporated, but is strongly dependent on its conformation.

2 Introduction

Reactive oxygen species (ROS) are pervasive throughout the cellular environment as byproducts of cellular functions, such as metabolism.¹⁻³ It plays a role in cell signalling,⁴⁻⁶ but due to its reactive nature, often interacts and damages critical cell infrastructure such as proteins and DNA.^{7,8} While all nucleobases are susceptible to ROS, oxoguanine remains the most stable and prevalent product of oxygen damage on DNA nucleobases.⁸ This forms around $1-2 \times 10^3$ lesions a day in healthy human cells^{8,9} with an increase in frequency in cancer cells.¹⁰ While repair mechanisms exist to detect and repair damaged nucleobases, these functions decline with age, and oxoguanine becomes a biomarker for an increasing risk of cancer.⁸

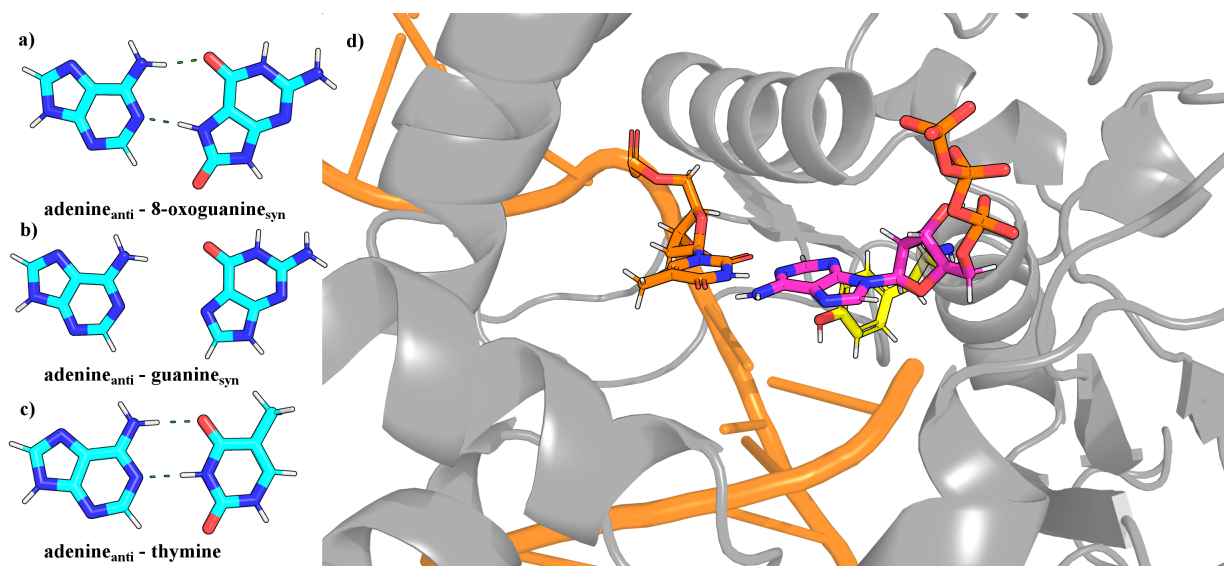


Figure 1: **a)** adenine in an anti conformation and 8-oxoguanine in the syn conformation paired together. **b)** adenine in an anti conformation and guanine in the syn conformation. **c)** adenine and thymine in an anti-canonical Watson-Crick pair. **d)** shows the polymerase-λ, 3PML,¹¹ with its active site, highlighted in green, showing the triphosphate structure pairing with the template strand. All three of the listed pairs are tested in this active site.

Mitochondria are a primary site of ROS production due to their metabolic activity.^{3,12} Since mitochondria contain their own DNA and undergo independent replication, they are particularly vulnerable to oxidative stress. ROS, generated as metabolic byproducts with mitochondria,¹² can readily react with DNA bases, leading to misincorporation during replication.

The difference between 8-oxoguanine and regular guanine lies in the presence of an electronegative oxygen atom that points towards the sugar backbone, creating both electrostatic and steric repulsion between itself and the sugar backbone.^{13–15} This indirectly creates a preference for a Hoogsteen conformation of 8-oxoguanine. When shifted to a Hoogsteen conformation, the additional oxygen no longer points to the backbone but is involved in hydrogen bonding between the DNA nucleobase pair.

While the steric and electrostatic disruptions to Watson-Crick bonding are significant, they are insufficient to cause an immediate shift to Hoogsteen pairing due to the presence of a substantial barrier (0.41 eV to 0.61 eV^{16,17}) between the two conformations.

When in the Hoogsteen conformation, the 8-oxoguanine can mismatch with adenine, with its hydrogen bonding surface pairing with adenine, mimicking the surface of thymine (see Figure 1), creating a source of point mutations. While a double purine bond would be rejected by the polymerase enzyme during replication, the pair usually forms a thymine mimicry¹⁸ that allows the misincorporated base pair to appear as a normal WC base pair and, in theory, move past the polymerase enzyme.

Experimental evidence supports the existence of 8-oxoguanine-adenine mimicry of a Watson-Crick base pair as a source of point mutation in the DNA chain.¹⁹ Stephanie *et. al.* have shown population estimates via experimental evidence using kinetic models in DNA chains with an 84 % population overall for all conformational structures of 8-oxoguanine paired with adenine.¹⁹ With a strong preference for a mutagenic pairing existing in the DNA chain, the question arises whether such a structure could survive polymerase and be misincorporated, potentially leading to further mutations.

However, the polymerase has additional protections against oxygen stress-related damage. It is known that the protein residue Tyrosine^{20,21} can disrupt the pairing of 8-oxoguanine, thereby helping to protect the DNA base against point mutation via misincorporation. The mutation

of this residue results in a significant increase in thumb closing time, suggesting its importance in moderating nucleobase inclusion.²¹ Furthermore, the mutation of similar moderating protein residues increases the mutagenic oxygen-damaged nucleobases.²²

3 Methodology

Classical Molecular Dynamics (MD) calculations were performed via GROMACS 2021.1.²³ The MD trajectories were set up with a polymerase enzyme actively forming a new DNA chain from the PDB structure 3PML.¹¹ The structure was set up using GROMACS from an input PDB file, which served as the basis for this investigation from a molecular dynamics (MD) viewpoint. All MD calculations focus on the polymerase’s active site, with no restraints added.

8-oxoguanine added as either the triphosphate or the template strand structure was parameterised using the CHARMM GUI²⁴ with the ligand reader to create forcefield parameters for use with the CHARMM 36 forcefield via GROMACS.^{23,25,26} MD calculations at a constant number of atoms, volume, and temperature (NVT ensemble) were performed on production MD to investigate the structure at a temperature of 310 K. Solvent effects were accounted for via an explicit solvent model via the TIP3P force field.²⁷ We ran the structure 100 times each for 2 ns, starting from the same energy-minimised structure for each system with a 0.5 fs timestep.

For comparison, we also set up and ran a standard DNA mispairing, matching the oxygen-stressed sequence but replacing it with a standard A-G pairing to observe the difference between the structures and ensure our definition of misincorporation was accepted. To define the misincorporation in the polymerase, we assume a DNA pairing in the active site, which can match the backbone spacing of an A-T WC nucleobase pair, would be able to move past the thumb closing mechanism of the polymerase enzyme, and be successfully misincorporated. This backbone spacing for an ‘ideal’ mispairing was set at 1.05 nm, and structures which maintained a spacing around this size were accepted as potential misincorporation structures. The comparison was made between the following structures, following the triphosphate nucleobase and the template strand nucleobase, respectively: 8-oxoguanine-adenine, adenine-8-oxoguanine, guanine-adenine, and adenine-guanine. The guanine assumed a Hoogsteen conformation in all cases, while the adenine remained in a standard Watson-Crick (WC) conformation.

Finally, we used the DNA chain in the 3PML structure to construct a B-DNA strand containing the 8-oxoguanine misincorporation. We have included this as a separate calculation to demonstrate the stability of 8-oxoguanine when misincorporated into the DNA strand and to directly compare it with experimental results. This DNA strand was run with the same parameters as the polymerase- λ MD calculation. Still, it included a salt concentration of 0.15 mol/litre to mimic the ion environment of DNA and balance the charges. We ran 20 separate structures for 10 ns each and plotted the backbone spacing to compare to experimental results.

4 Results and Discussion

4.1 Molecular Dynamics Investigations of 8-oxoguanine paired in a B-DNA chain

To compare to experimental results,¹⁹ we investigated interactions and stability of 8-oxoguanine in a B-DNA structure surrounded by an aqueous solvent. QM calculations decided the mispair conformation (see SI for details).

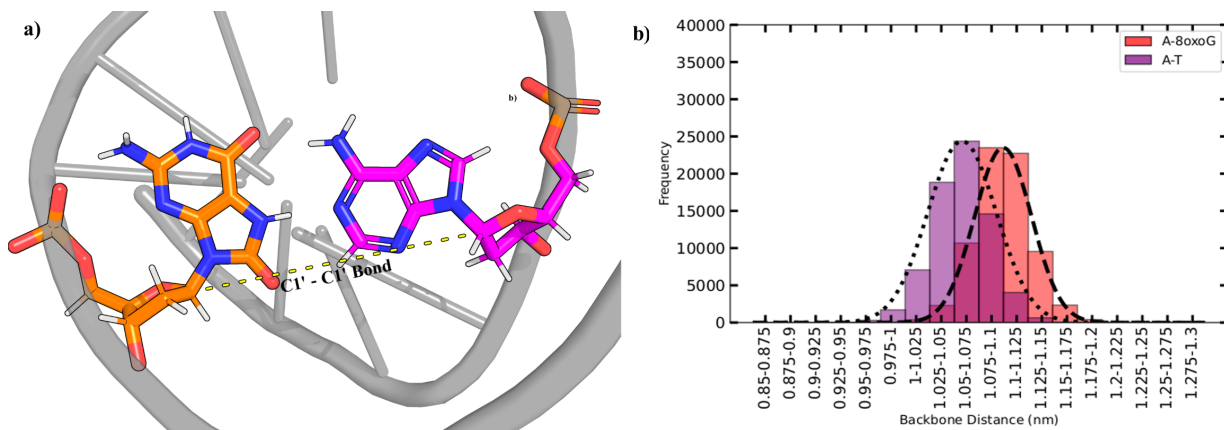


Figure 2: **a)** 8-oxoguanine_{syn} bonded with an adenine inside DNA. Marked is the backbone spacing between the C1' carbons at the backbone of each nucleobase. This is our measurement of backbone spacing. **b)** histogram of all recorded backbone spacings between adenine-8-oxoguanine pair compared to the backbone spacing of the canonical adenine-thymine pair while in DNA. This represents 20 10 ns MD simulations of the B-DNA chain in solution.

We can clearly see that 8-oxoguanine is stable when occupying the Hoogsteen bonding while adopting the syn conformation as seen in Figure **a** and **b** 2. The histograms show little variation between backbone spacing, with comparable distribution between the adenine-8-oxoguanine structures and the canonical adenine-thymine structures across 10 ns of simulation. We did not observe any significant conformational change that would indicate transitions between WC-like and Hoogsteen pair conformations, demonstrating that the pair remains stable within our simulation time. This is not surprising, as the time scales for Hoogsteen inversion are on the order of milliseconds.¹⁹

Compared to experimental results and our results, Stephanie *et. al.*¹⁹ have measured the 8-oxoguanine syn backbone spacing for C1'-C1' to be (10.4 ± 0.5) Å with adenine-thymine equivalent spacing at 10.5 Å. Our MD results show a slightly larger average spacing for 8-oxoguanine with a density peak at 11.00 Å versus a density peak of 10.58 Å as seen in Figure 2 **a**). Our results fall outside of the error margin proposed by the experimental values for C1'-C1' backbone spacing; however, compared to the standard deviation error, the peak of our results falls within the error of the experimental results with an error of 0.284 Å to the density peak of 11.00 Å.

Despite this, the N-N backbone spacing from adenine-8-oxoguanine is nearly identical to that of adenine-thymine. adenine-8-oxoguanine has a density peak at 9.01 Å compared to a density peak for adenine - thymine of 8.87 Å. They maintain a similar spacing as seen in Figure 2 **b**. Why exactly the backbone spacing seems to act differently is unclear currently, but potential steric reactions with the -NH₂ structure, originally part of the electronegative Watson-Crick site, pointing out towards the solvent, may interact with the backbone and shift it out of position.

4.2 Investigating the Misincorporation Dynamics of 8-oxoguanine at the Active Site of Polymerase λ

We employ molecular dynamics to investigate the role of the surrounding polymerase λ environment when interacting with the adenine-8-oxoguanine mispair. Understanding how polymerase affects the stability of the mispair at the active site is crucial in determining its ability to be misincorporated by the polymerase. We utilise the x-ray structure 3PML¹¹ to simulate the surrounding polymerase structure and replace the DNA bases at the active site with an adenine-8-oxoguanine pair. Based on the QM results (see SI), the conformation of the A_{anti}-8-oxoG_{syn} structure has the tightest binding and thus the most stable. This was taken as the conformation to be simulated in the polymerase. By comparing the backbone spacing between the C1'

atoms of each nucleobase, we can determine the similarity between the misincorporation and the canonical base pair. We tested the difference for four cases: A_{anti} -8-oxoG_{syn} on the triphosphate and template strand respectively, and the reversed structure, and to compare if our definition of binding is correct, A_{anti} -G_{syn} on the triphosphate and template strand respectively.

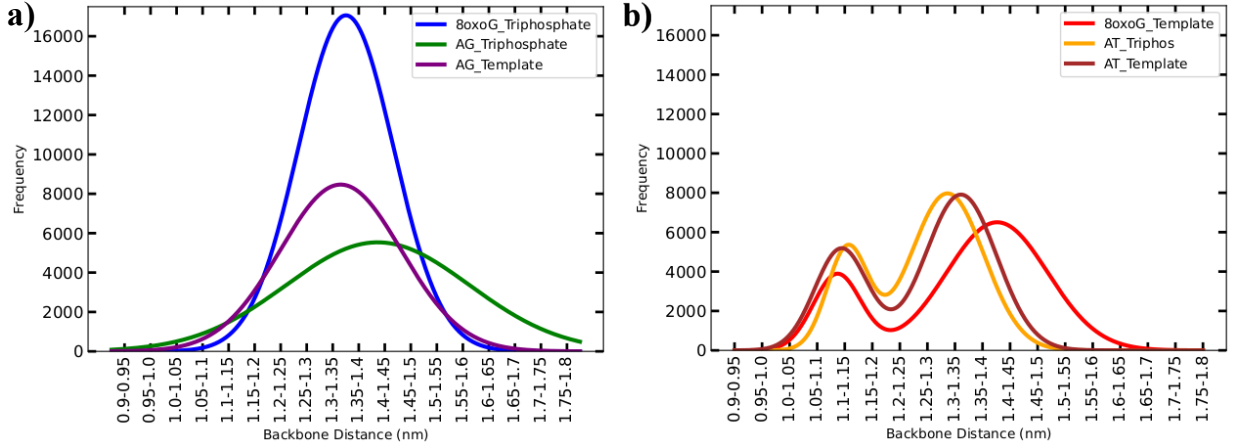


Figure 3: Density line plots covering all simulated structures backbone C1'-C1' distance at the active site of polymerase λ . **a)** shows the adenine-8-oxoguanine triphosphate and adenine-guanine triphosphate and template structures. **b)** shows the adenine-8-oxoguanine template and the adenine-thymine control triphosphate and template structure. It is shown how similar the 8-oxoguanine located on the template structure is to the canonical adenine-thymine pair. Each density plot is a range over 100 MD calculations, each 2 ns long, taken from the final 1 ns (See the SI and Figure S1 for more information on these density plots).

We observe in the above Figure a wide distribution of C1'-C1' backbone spacings across all simulations, with Figure **a)** 3 exhibiting a spike in interaction around 1.3 Å due to the surrounding polymerase structure, primarily focused on the Tyrosine 251 residue. We observe a clear similarity in trend between the two control structures, of adenine and thymine paired in the polymerase with the oxygen-damaged misincorporated template strand 8-oxoguanine, in the syn conformation as seen in Figure **b)** 3. Comparing the peaks of the Gaussian lines in the right graph, we get a peak of 1.111 nm, 1.130 nm, 1.119 nm for Template 8-oxoguanine, thymine triphosphate, and template, respectively, which are a similar match to the DNA strand spacing.

The density line indicates 8-oxoguanine is still disrupted by the polymerase and tyrosine, with a smaller peak when compared to the canonical adenine-thymine pair. However, 8-oxoguanine, while connected to the template DNA strand, can mimic adenine-thymine canonical pairing inside polymerase λ . This provides strong support for misincorporation via 8-oxoguanine being treated as a thymine by the polymerase, but shows that the location of 8-oxoguanine is critical to allow its misincorporation. 8-oxoguanine located on the triphosphate structure is significantly disrupted by Tyrosine 251 in polymerase λ as seen in Figure 3 **a)**. This, we believe, is due to a 'wedging' mechanism via Tyrosine 251.

4.3 Wedge Interaction between Tyrosine 251 and the Mutagenic Hoogsteen Mismatch with 8-oxoguanine

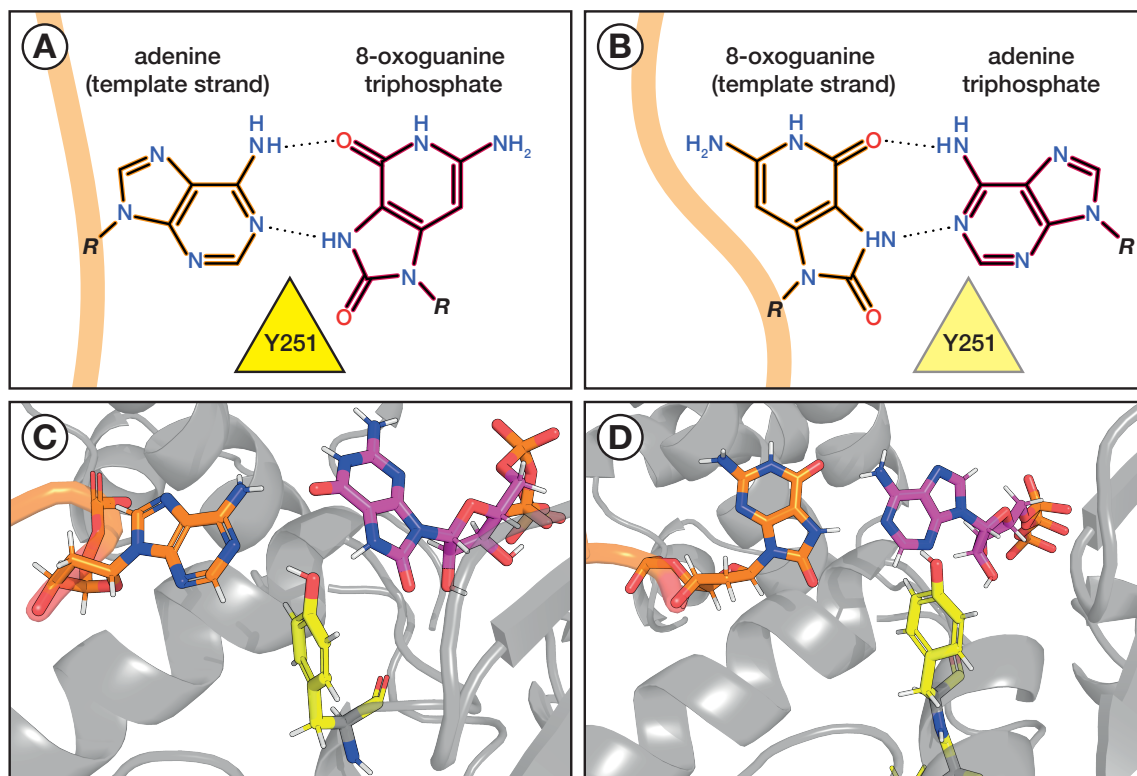


Figure 4: Structure of the wedge mechanism interacting with adenine-8-oxoguanine Hoogsteen mismatch at the active site of polymerase λ . **A** Schematic Figure of the mismatch with protein residue aligned to 'wedge' between adenine and 8-oxoguanine located on the triphosphate. **B** Schematic Figure of the mismatch with protein residue misaligned to 'wedge' between adenine and 8-oxoguanine located on the template strand. **C, D** Visual structure of the 'wedge' mechanism from MD simulations of the mismatch at the active site of polymerase λ with the 8-oxoguanine triphosphate structure and the 8-oxoguanine template structure.

The 'wedging' mechanism is located in the polymerase active site (see Figure 4 and Figure 3 a)). The protein residue Tyrosine 251 is positioned to sit between the adenine and 8-oxoguanine structures as they connect. When the 8-oxoguanine mimics the purine structure on the triphosphate, the gap with adenine is aligned with the tyrosine 251. This allows the tyrosine to move between the two structures, seemingly attracted by the electronegative oxygen acceptor near the protein residue attached to 8-oxoguanine and hydrogen bond to it. The oxygen at the end of the tyrosine then bonds to the corresponding hydrogen located on adenine, which was initially intended to bond to the 8-oxoguanine. This causes the protein residue to sit between the two nucleobases, maintaining a connection between the two structures and disrupting the inclusion of this misincorporation, thereby delaying or preventing thumb closing from occurring.

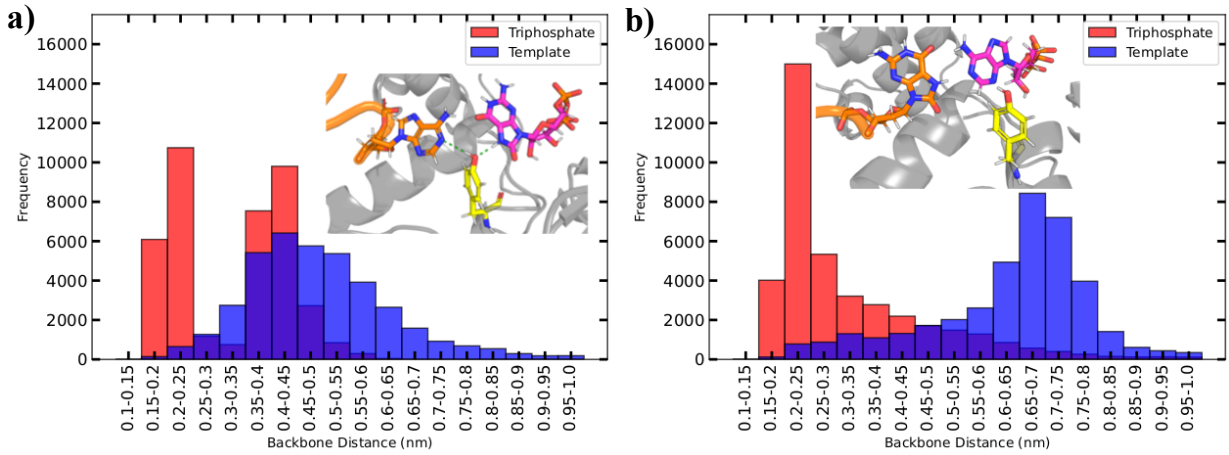


Figure 5: Results comparing the hydrogen bond distance between tyrosine 251 and the nearby misincorporation pair depending on the location of 8-oxoguanine. **a)** shows the hydrogen bond distance between adenine and tyrosine, comparing the template and triphosphate 8-oxoguanine. **b)** shows the hydrogen bond distance between 8-oxoguanine and tyrosine, comparing the template and triphosphate 8-oxoguanine.

We observe spikes at hydrogen bonding distances across both graphs, indicating a strong preference for the spacing between Tyrosine and 8-oxoguanine in the triphosphate conformation, as shown in Figure 5 **b)**. However, across the simulation, adenine can shift, as seen in Figure 5 **a)**, where the adenine hydrogen bond length exhibits two prominent peaks in its distribution. This is potentially due to the electronegative binding surface of 8-oxoguanine compared to adenine. The oxygen positioned near the backbone is an attractive surface for tyrosine 251 to hydrogen bond to, allowing it to move deeper into the structure. This gives a clear preference towards 8-oxoguanine, and hydrogen bonding to adenine is a consequence.

However, when the 8-oxoguanine is located on the template strand, the position of the hydrogen bonds between the nucleobases is slightly shifted. This slight shift moves it out of line with tyrosine 251 and reduces its impact on disrupting the binding of 8-oxoguanine. No longer as aligned as the triphosphate structure (see Figure 4, the misincorporated base pair can now achieve a suitable backbone spacing to mimic a standard A-T base pairing more frequently (see Figure 3), with the first peak of backbone spacing around 1.0 - 1.05nm. Still, due to the slight misalignment of the hydrogen bond gap, the structure is pushed further apart as the tyrosine disrupts the binding. Due to the difference in spacing between the purine and pyridine mimic structures of 8-oxoguanine syn and tyrosine, the latter cannot disrupt as effectively when 8-oxoguanine is located on the triphosphate structure. This suggests that the location of 8-oxoguanine is crucial to its incorporation.

When comparing the hydrogen bonds between Tyrosine 251 and 8-oxoguanine - adenine while located on the template strand, we see a significantly broader range of hydrogen bonding distances, with the average trend being beyond a maximum hydrogen bond distance (which we define as 3.3 Å) in Figure 5 **b)**. Compared to the triphosphate data, this significant drop in bonding helps indicate the reduction in disruption via Tyrosine 251. Tyrosine 251 can still disrupt the structure, as indicated in Figure 5 **a)**, with a non-negligible interaction with adenine. However, due to its significantly reduced hydrogen bonding with 8-oxoguanine, its location on the template strand helps shield it from this fidelity check.

However, let us compare the simulations to the performance of the same polymerase, where the oxygen-damaged guanine is swapped for an undamaged guanine, Figure 3. We see a wider spread of results across the structure with no clear indication of significant disruption, such as the large spike in Figure 3 from 8-oxoguanine triphosphate. The majority of structures, including guanine, have larger backbone spacing than the ideal 1.05 nm and don't match the

data trend shown in either 8-oxoguanine structures or thymine structures. We observe that some structures have a backbone spacing of approximately 1.05 nm. Upon investigation, this was found to be due to the formation of a Hoogsteen structure between adenine and guanine, where the nucleobase pairs were misaligned. There was little interaction between tyrosine 251 due to the lack of attractive hydrogen binding sites to connect to. Most structures fail to form a strong connection due to the lack of available hydrogen bonds and drift apart or move into a misaligned pairing state.

Compared to the controls, replacing 8-oxoguanine with thymine in the syn position shows a peak Gaussian at 1.130 nm and 1.119 nm for the triphosphate and template, respectively. These structures are nearly identical in trend and data spread and are affected by Tyrosine 251 identically. When compared to Figure 3, 8-oxoguanine performs similarly to the canonical pair in the polymerase λ environment to thymine while located on the template strand.

With all the data from the MD simulations, we see a clear pathway for misincorporation via a high-fidelity polymerase structure for 8-oxoguanine. The structure maintains a similar C1' backbone spacing to that of an adenine-thymine Watson-Crick pair, effectively mimicking its structure. While our results suggest that 8-oxoguanine while located in a B-DNA chain has a higher than average backbone spacing at 1.1 nm than adenine - thymine at 1.05 nm and is just out from the experimentally predicted spacing of (1.04 ± 0.50) nm, 1.1 nm spacing seems to be the standard spacing while located in the polymerase λ of which our results, when running the same forcefield and parameters, match both 8-oxoguanine and adenine - thymine. This indicates that the structure can bypass polymerase λ and move past the thumb, closing to be misincorporated into the DNA chain, allowing a point mutation to occur. It is known that further fidelity checks via Oxoguanine glycosylase (OGG1)²⁸ along the chain can detect and repair 8-oxoguanine, which may rely on a slight shift in conformation due to a larger backbone spacing to detect 8-oxoguanine even while mimicking the Watson-Crick pair.

5 Conclusion

In conclusion, 8-oxoguanine can mimic the canonical adenine-thymine WC pair and achieve a suitable conformation to move past the fidelity of polymerase- λ . QM models demonstrate a preference for 8-oxoguanine to maintain a Hoogsteen conformation with the 8-oxoguanine inverting to disguise its conformation as thymine, allowing adenine to bond to it and achieve similar backbone spacing. MD demonstrates how the polymerase- λ disrupts oxygen-damaged nucleobases, with Tyrosine 251 playing a key role in splitting the 8-oxoguanine inclusion into the DNA chain, especially when bound to the triphosphate structure, forming a wedge structure that pushes apart the nucleobases and disrupts the thumb closure of polymerase λ . However, the effectiveness of this mechanism is reduced when 8-oxoguanine is located on the template strand of DNA.

These results help show how experimental results find the stable mutagenic 8-oxoguanine form bound in a Hoogsteen state to adenine. Stephanie et al. showed the stability and population of the mutagenic pair in a DNA chain. Our computational results further show how such mutagenic structures can form naturally in cells and occur in the DNA chain. As the high-fidelity polymerase λ can not fully filter 8-oxoguanine misincorporation, these mutagenic pairs can enter the system and remain stable inside DNA until either helicase replicates the chain, causing the point mutation, or a repair mechanism removes the 8-oxoguanine in the chain.

Further repair mechanisms, such as OGG1,²⁸ could subsequently locate and correct the 8-oxoguanine error, and future work could be performed to investigate the lifetime of 8-oxoguanine after it has been successfully misincorporated via polymerase. Suppose the 8-oxoguanine misincorporation is not detected before the DNA chain is replicated. In that case, it will create a point mutation, as subsequent structures will replace the cytosine-guanine structure with an

adenine-thymine pair. Further work could also investigate the role of the above DNA nucleobases as they are incorporated into the DNA chain via polymerase. Tyrosine 251 interacts and bonds to the above DNA nucleobase from the active site before moving to disrupt 8-oxoguanine. The strength of this bond could also play a key role in the misincorporation of 8-oxoguanine.

Author Contributions

G. F. MD and DFT calculations, analysis, and conceptual development.

L. S. supervision, conceptual development, and project conceptualisation.

M. W. assistance with MD parameterisation and preparation.

B. H. supervision and conceptual development.

M. S. supervision and conceptual development.

All authors contributed to the writing and development of the paper.

Conflicts of Interest

There are no conflicts to declare.

Acknowledgements

M.S. is grateful for support from the Royal Society (URF/R/191029). The authors thank the ARCHER2 UK National Supercomputing Service. This work was supported by HECBioSim, the UK High-End Computing Consortium for Biomolecular Simulation, funded by EPSRC (EP/L000253/1). L. S. thanks the Beyond Center for funding. We also want to extend our condolences to Prof. Brendan Howlin’s family, friends, and colleagues. His insights and genuine passion for research will be greatly missed.

Data Availability

The data and code associated with this study are freely available on Github.

AI Disclosure

Portions of the data analysis code were generated with the assistance of GitHub Copilot. The authors utilised Grammarly and OpenAI ChatGPT-4o for minor grammatical and stylistic suggestions during manuscript preparation. The tool was not used to generate any original scientific content or citations. All suggestions were critically reviewed, edited, and verified by the authors. All edits were reviewed and incorporated at the authors’ discretion. The authors are responsible for the final code, data interpretation, and the content of the manuscript. The AI tool is not listed as an author and did not contribute to the interpretation of the study results.

References

- [1] Pereira, E. J.; Smolko, C. M.; Janes, K. A. *Frontiers in Pharmacology* **2016**, Volume 7 - 2016.

- [2] Gowder, S. J. T. *Basic principles and clinical significance of oxidative stress*; BoD–Books on Demand, 2015.
- [3] Lambert, A. J.; Brand, M. D. *Mitochondrial DNA: methods and protocols* **2009**, 165–181.
- [4] Thannickal, V. J.; Fanburg, B. L. *American Journal of Physiology-Lung Cellular and Molecular Physiology* **2000**, *279*, L1005–L1028.
- [5] Rhee, S. G. *Experimental & molecular medicine* **1999**, *31*, 53–59.
- [6] Finkel, T. *Current opinion in cell biology* **1998**, *10*, 248–253.
- [7] Davies, M. J. *Biochemical journal* **2016**, *473*, 805–825.
- [8] van Loon, B.; Markkanen, E.; Hübscher, U. *DNA Repair* **2010**, *9*, 604–616.
- [9] Yudkina, A. V.; Shilkin, E. S.; Endutkin, A. V.; Makarova, A. V.; Zharkov, D. O. *Crystals* **2019**, *9*, 269.
- [10] Nakabeppu, Y. *International journal of molecular sciences* **2014**, *15*, 12543–12557.
- [11] Bebenek, K.; Pedersen, L. C.; Kunkel, T. A. *Proceedings of the National Academy of Sciences* **2011**, *108*, 1862–1867.
- [12] Palma, F. R.; Gantner, B. N.; Sakiyama, M. J.; Kayzuka, C.; Shukla, S.; Lacchini, R.; Cuniff, B.; Bonini, M. G. *Oncogene* **2024**, *43*, 295–303.
- [13] Geronimo, I.; Vidossich, P.; De Vivo, M. *Journal of Chemical Information and Modeling* **2023**, *63*, 1521–1528, PMID: 36825471.
- [14] Tomáš, D.; Mahmut, K.; Martin, Z.; Filip, L. *The Journal of Physical Chemistry B* **2013**,
- [15] Ovcherenko, S. S.; Shernyukov, A. V.; Nasonov, D. M.; Endutkin, A. V.; Zharkov, D. O.; Bagryanskaya, E. G. *Journal of the American Chemical Society* **2023**, *145*, 5613–5617.
- [16] Chakraborty, D.; Wales, D. J. *The Journal of Physical Chemistry Letters* **2018**, *9*, 229–241, PMID: 29240425.
- [17] Yang, C.; Kim, E.; Pak, Y. *Nucleic acids research* **2015**, *43*, 7769–7778.
- [18] Hahm, J. Y.; Park, J.; Jang, E.-S.; Chi, S. W. *Experimental & molecular medicine* **2022**, *54*, 1626–1642.
- [19] Gu, S.; Szymanski, E. S.; Rangadurai, A. K.; Shi, H.; Liu, B.; Manghrani, A.; Al-Hashimi, H. M. *Nature Chemical Biology* **2023**, *19*, 900–910.
- [20] Wang, Y.; Reddy, S.; Beard, W. A.; Wilson, S. H.; Schlick, T. *Biophysical journal* **2007**, *92*, 3063–3070.
- [21] Wang, Y.; Schlick, T. *BMC structural biology* **2007**, *7*, 1–14.
- [22] Brieba, L. G.; Kokoska, R. J.; Bebenek, K.; Kunkel, T. A.; Ellenberger, T. *Structure* **2005**, *13*, 1653–1659.
- [23] Berendsen, H.; van der Spoel, D.; van Drunen, R. *Computer Physics Communications* **1995**, *91*, 43–56.

- [24] Jo, S.; Kim, T.; Iyer, V. G.; Im, W. *Journal of Computational Chemistry* **2008**, *29*, 1859–1865.
- [25] Huang, J.; MacKerell Jr, A. D. *Journal of computational chemistry* **2013**, *34*, 2135–2145.
- [26] Brooks, B. R. et al. *Journal of Computational Chemistry* **2009**, *30*, 1545–1614.
- [27] Mark, P.; Nilsson, L. *The Journal of Physical Chemistry A* **2001**, *105*, 9954–9960.
- [28] Nishioka, K.; Ohtsubo, T.; Oda, H.; Fujiwara, T.; Kang, D.; Sugimachi, K.; Nakabeppu, Y. *Molecular biology of the cell* **1999**, *10*, 1637–1652.